Flow of nanosize cluster-containing plasma in a magnetron discharge

Boris M. Smirnov,[1] Ibrahimkutty Shyjumon,[2] and Rainer Hippler[2,*]
[1]*Institute for High Temperatures, Russian Academy of Sciences, Izhorskaya 13/19, Moscow 125412, Russia*
[2]*Institut für Physik, Ernst-Moritz-Arndt-Universität Greifswald, Felix-Hausdorff-Strasse 6, 17489 Greifswald, Germany*
(Received 21 December 2006; revised manuscript received 24 April 2007; published 22 June 2007)

A magnetron source of silver clusters captured by an argon flow with the quadrupole mass filter is used for the analysis of charged clusters after an orifice of the magnetron chamber, and the size distribution function follows from the analysis of clusters deposited on a silicon substrate by an atomic force microscope. Cluster charge near an orifice results from attachment of ions of a secondary plasma that is a tail of a magnetron plasma, and the cluster charge is mostly positive. The character of passage of a buffer gas flow with metal clusters through an orifice is studied both theoretically and experimentally. Assuming the cone shape of the drift chamber near the orifice, we analyze drift of charged clusters in a buffer gas flow towards the orifice if the electric field inside the drift chamber is created by charged rings on the cone surface. Under experimental conditions, when an equilibrium between the buffer gas flow and cluster flux is violated, a typical voltage of rings and parameters of corona discharge for cluster charging are estimated if the electric field does not allow for clusters to reach walls of the drift chamber. The number density of clusters near the orifice is estimated that increases both due to violation of an equilibrium for the cluster flux inside the buffer gas flow and owing to focusing of the cluster by the electric field that is created by electrodes located near walls and due to diffusion motion of clusters. Processes of cluster charging in the magnetron chamber are analyzed.

DOI: 10.1103/PhysRevE.75.066402 PACS number(s): 52.25.Fi, 52.77.Dq

I. INTRODUCTION

As metal clusters are formed from metal atoms it is necessary, for generation of metal clusters from a solid material, to convert also a condensed metal into a metal vapor [1–3]. Along with the standard conversion method by laser evaporation [4–7], it is convenient to use for this goal a magnetron discharge [8–11], where metal atoms result from bombardment of the cathode by ions of a buffer gas with kinetic energy of several hundred eV. One more advantage of magnetron discharge is a uniformity of the discharge current at a large cathode dimension that allows one to produce metal atoms in a large volume. Such large dimensions of magnetron discharge provide the possibility to prevent metal atoms from their attachment to walls in spite of a low pressure of a buffer gas. Therefore, the magnetron method is useful for production of metal atom beams and cluster beams.

Because of the large dimensions of a magnetron chamber, metal atoms located not close to the cathode are converted into clusters effectively. These metal clusters are captured by a slow flow of a buffer gas and are removed in this way from the region of their formation. But because of a low pressure in the magnetron chamber, times of establishment of various equilibriums are large in the magnetron chamber. Being guided on improving yield parameters of the magnetron cluster source, that can be based on study and knowing processes in the magnetron cluster plasma, we concentrate below on these processes far from the cathode, involving the orifice region. These processes are similar both for stationary and radio-frequency magnetron cluster source [12] and lead to specific equilibria both for a plasma flow with clusters. The behavior of such a magnetron cluster plasma is a topic of this paper.

*Author to whom correspondence should be addressed; hippler@physik.uni-greifswald.de

In particular, the drift velocity of clusters differs from the velocity of a buffer gas when a buffer gas leaves the magnetron chamber through an orifice. The nonequilibrium character of processes involving clusters, on the one hand, makes these processes more complicated in reality, and, on the other hand, allows us to govern these processes in order to obtain the optimal conditions for cluster transport. These problems are the topic of this paper.

The main problem under consideration here is to increase the metal flux transported in magnetron discharge from the cathode to a target. Magnetron discharge provides metal erosion on a large cathode area that allows one to obtain a high rate of generation of metal atoms. But because of the small gas pressure in magnetron discharge and the relatively large diffusion coefficient of atoms, metal atoms generated in a magnetron discharge cannot be transported over large distances, since then metal atoms attach to walls of the magnetron chamber. If atoms are converted into clusters, their attachment to walls will be reduced because of small diffusion coefficient of clusters. But near the orifice the probability for a neutral cluster to attach to walls is not small, while charged clusters are repulsed from the walls due to the wall voltage. We analyze below this possibility being guided by silver clusters which are moving in an argon flow. The experimental results help us to extract the main processes of growth and transport of metal clusters. The theoretical analysis allows us to ascertain the possibilities of this method for metal transport and requirements related to the experiment.

II. EXPERIMENTAL SETUP AND SOME RESULTS

A general scheme of the aggregation chamber with magnetron discharge is given in Fig. 1, where the magnetron chamber is given. The target atoms are produced by direct current (dc) magnetron sputtering. Clusters are formed by the attachment of free atoms and coagulation process [2,11] in-

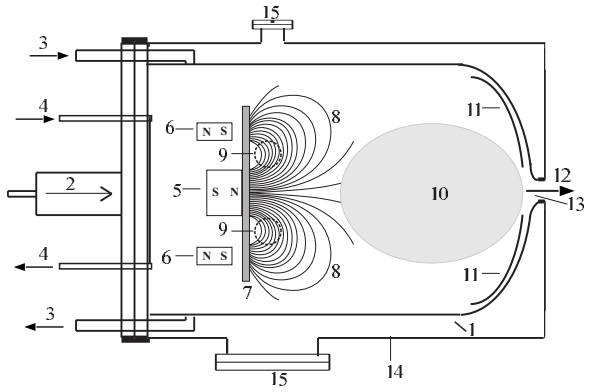

FIG. 1. Aggregation chamber (schematic): 1, aggregation chamber; 2, flow of buffer gas; 3, liquid nitrogen for cooling of the chamber; 4, water for magnetron cooling; 5, internal cylindrical magnet; 6, external ring magnet; 7, cathode; 8, magnetic lines of force; 9, ring of captured electrons (race track); 10, secondary plasma; 11, electrode for secondary plasma; 12, flow of buffer gas with clusters; 13, orifice; 14, outer chamber; 15, pumping port.

side the liquid-nitrogen (L-N_2) cooled aggregation tube of variable length that is based on a concept developed by Haberland *et al.* [13–15]. These clusters flow together with the carrying gas (Ar) through a variable orifice with a typical diameter of 3 mm. After the orifice these clusters can be mass selected by a quadrupole mass filter, followed by charge separation with the help of an extraction unit.

The cathode is a disc of typical diameter of 50.8 mm (2 in.), its maximum thickness is 5 mm, and is surrounded by a target holder which serves as the anode. When a sufficiently large dc voltage is applied, a discharge occurs nearby the cathode which ionizes the Ar atoms and these Ar ions sputter out the target material. Electrons are locked by the magnetic field and move in a ring (race track) as it is shown in Fig. 1, as the drift of electron motion is perpendicular to both electric and magnetic fields [16,17].

In the quadrupole mass filter clusters can be selected with respect to their mass-charge ratio by the quadrupole electric field, so that only ions of a certain mass M will be transmitted [18]. The motion of ions inside the quadrupole field is described by the Mathieu equation [19]. The mass selection is controlled by the frequency f (kHz) and the amplitude of ac voltage V_{ac} (in volts) as given by

$$M = 7 \times 10^7 k \frac{V_{ac}}{f^2 d^2}, \tag{1}$$

where M is the cluster mass in atomic mass units (amu), $d = 25.4$ mm is the rod diameter, and k is a correction factor of the order of unity. The extraction unit that follows the mass filter consists of a set of circular electrodes, and by choosing a proper polarity at these electrodes enables us to select only one type of charged clusters (we selected only positively charged clusters for this study by applying an extraction voltage of −700 V). Finally, these clusters are deposited on a Si(100) substrate that is kept at a distance of about 53 cm from the exit of the magnetron chamber.

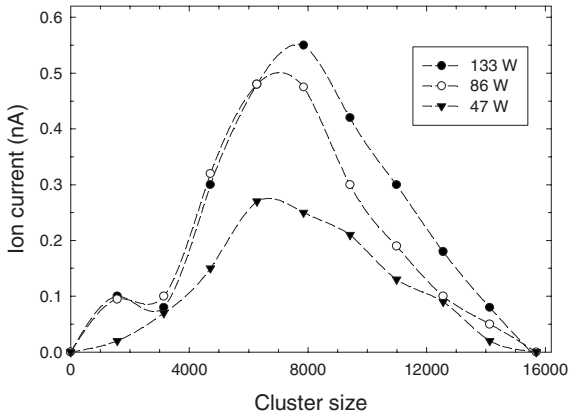

FIG. 2. Cluster size distribution as measured with the quadrupole mass filter for different magnetron discharge powers [pressure 0.12 mbar, argon gas flow 12.5 sccm (standard cubic centimeter per minute), wall temperature 173 K].

The processes of formation and growth of clusters near the silver cathode of magnetron discharge in an argon flow are identical to those in the case of the titanium cathode which we analyzed in our previous work [11]. As before, we use atomic force microscopy (AFM) for the analysis of the size distribution function of clusters deposited on a substrate [11]. Along with the atomic force microscope we select clusters in a narrow range of sizes by a quadrupole mass filter [18]. Figure 2 displays the cluster mass distribution for different magnetron discharge powers as measured with the mass filter (also see Fig. 3). It is noted that the mass distribution peaks around a mean cluster size $n \approx 7000$ atoms/cluster. The dependence of the mean cluster size corresponding to the maximum of the size distribution function (in the following we consider it as the average or mean cluster size) as a function of magnetron discharge power is displayed in Fig. 4. Ignoring a weak power dependence, the average cluster size is approximately independent of the discharge power

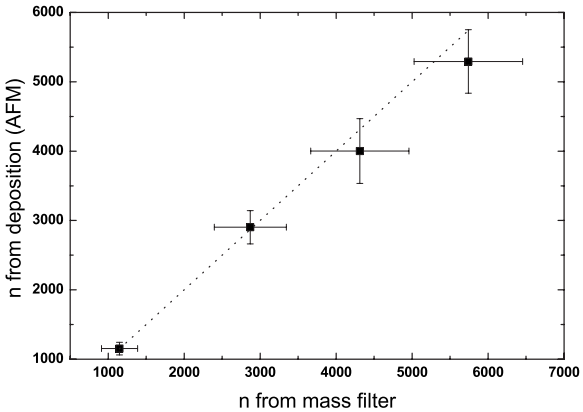

FIG. 3. Average cluster size (n is an average number of cluster atoms corresponding to the maximum of the size distribution, see Fig. 2) as obtained with the help of a quadrupole mass filter versus size of deposited clusters derived by AFM measurement. Experimental conditions: pressure inside magnetron chamber $p = 0.1$ mbar; gas flow 12 sccm (standard cubic centimeters per minute); wall temperature of magnetron chamber $T = 198$ K.

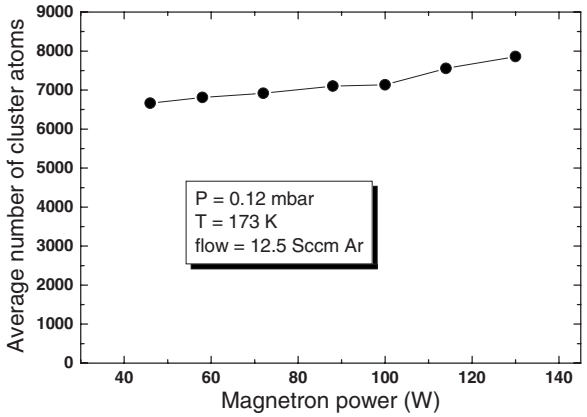

FIG. 4. Average cluster size (mean number of cluster atoms) versus power of magnetron discharge.

in the given range of parameters. Similar sizes of silver clusters have been observed by Pratontep *et al.* [12] employing a radio-frequency magnetron plasma sputtering source.

Figure 3 compares the average size of deposited clusters measured by AFM with the cluster size determined with the help of a mass filter [20]. Note that the magnetron cluster source under consideration gives a broad size distribution of clusters, while the quadrupole mass spectrometer allows for the selection of an adjustable and narrower mass range.

Also note that the measured silver cluster sizes are smaller by about one order of magnitude compared to the titanium case [11] under the same experimental conditions, i.e., argon pressure, pumping rate, and wall temperature. This can be explained by different values of the rate constant for the three-body process

$$\mathrm{Ag} + \mathrm{Ag} + \mathrm{Ar} \rightarrow \mathrm{Ag}_2 + \mathrm{Ar} \tag{2}$$

that leads to the formation of silver, respectively, titanium diatomic molecules which subsequently form the nuclei of cluster growth. Using the formula for the average cluster size n (we express here the cluster size as a number of bound cluster atoms) after conversion of an atomic vapor in clusters, we find the rate constant for the three-body process in the silver case to be $K_{\mathrm{Ag}}=5.5\times10^{-33}$ cm^6/s, whereas in the titanium case it is equal to $K_{\mathrm{Ti}}=2.5\times10^{-33}$ cm^6/s [11] at $T=200$ K. Note that under experimental conditions, silver clusters of a maximum size contain 2×10^4 atoms. After the nucleation process small clusters grow by atom absorption, e.g.,

$$\mathrm{Ag}_n + \mathrm{Ag} \rightarrow \mathrm{Ag}_{n+1}. \tag{3}$$

In addition, medium and large size clusters may coagulate to form even larger clusters,

$$\mathrm{Ag}_n + \mathrm{Ag}_m \rightarrow \mathrm{Ag}_{n+m}. \tag{4}$$

The reaction rate for this latter process would be greatly enhanced if electrical charging of clusters occurs and through interaction of clusters with opposite charge. The likeliness of nanosize particle charging was investigated by numerical simulation by Cui and Goree [21]. Accordingly, small particles (clusters) embedded in a plasma may display an appreciable charging depending on cluster size and electron temperature. The simulation shows that almost all clusters will be negatively charged and only a minor fraction of typically 10^{-3} or less should attain a positive charge. One may thus argue that under the given circumstances charging of clusters should be of little influence to cluster growth. However, these findings are not supported by experimental investigations which show that appreciable amounts of positively charged metal clusters are produced in magnetron-type cluster sources [11,12].

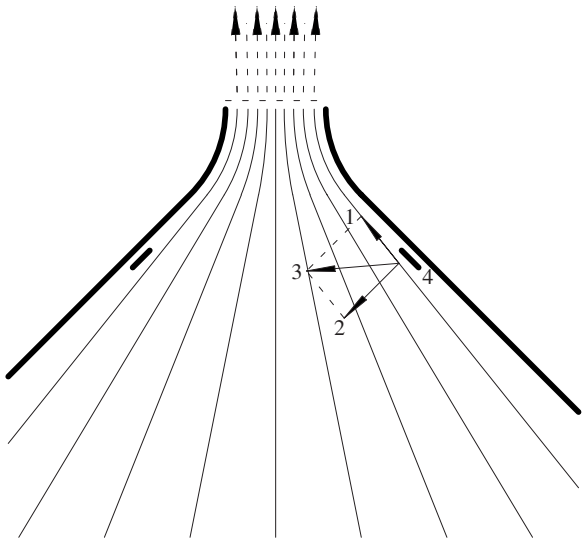

FIG. 5. The current lines for buffer gas flow inside a conic chamber near an orifice when the flow passes the orifice. 1, force acting on a cluster from a buffer gas flow; 2, force from an electric field; 3, total force acting on cluster; 4, ring electrode.

III. CHARACTER OF BUFFER GAS FLOW AND DRIFT OF CLUSTERS IN FLOW

The drift velocity of clusters when moving in a slow flow of a buffer gas coincides with the drift velocity of buffer gas atoms, i.e., equilibrium between the flowing gas and clusters is established. With increasing flow velocities the equilibrium between the drift velocities of flowing atoms and clusters may be violated, however. The drift velocity of buffer gas atoms near the orifice is of the order of the speed of sound, while the drift velocity of clusters is significantly smaller as the time to accelerate clusters to high speed becomes too short, and, hence, equilibrium conditions are difficult to reach near the orifice. This results in an increase of the cluster number density that can enforce their coagulation near the orifice if clusters are neutral.

In the following we shall analyze the processes involving clusters near the orifice. For simplicity we consider a conic shape of the magnetron chamber near the orifice and first analyze the gas flow in this region. Figure 5 gives the current lines for a gas near the orifice. As the total flux of atoms is conserved in each cross section of the cone chamber near the orifice, atoms of a buffer gas are moving on average along the straightforward current lines. The drift velocity of buffer gas atoms increases towards the orifice and creates a force

that acts on clusters and compels them to increase the drift velocity up to the gas drift velocity. However the establishment of an identical drift velocity for clusters and the gas flow requires a large time because of a large cluster mass, and these drift velocities are different near the orifice.

In addition we shall consider the case of charged clusters and the surface to have an electric potential. Taking this electric potential due to electrodes located on walls, and its action into account leads to repulsion of clusters from electrodes, i.e., we obtain an additional force to clusters. As a result, the final cluster beam is focusing in the end, and below we analyze these processes in detail being guided by the experimental conditions.

The reduced argon flow rate Q/Q_0, where $Q_0=N_0c_s\pi R_o^2$, N_0 is the number density of argon atoms inside the magnetron chamber, c_s is the speed of sound, R_o is the orifice radius, and with the flow rate Q expressed as $Q=N_0u_0\pi R_o^2$, was measured for the present experimental conditions (see Ref. [11]). The flow parameter $u_0\approx 0.84c_s$ as extracted from those measurements is largely independent (within ±10%) of both flow rate and orifice radius. For argon at a temperature of 200 K the speed of sound is $c_s=2.6\times 10^4$ cm/s and, hence, $u_0=2.2\times 10^4$ cm/s.

Let us consider the flow characteristics of a pure buffer gas in a cone-shaped chamber that terminates at an orifice. We denote the axis of this chamber by z with $z=0$ at the orifice having a radius R_o. The forward-directed current lines form a certain angle with the cone axis (see Fig. 5) and its maximum value for the chamber boundary we denote by α. Assuming the number density of a buffer gas to be constant inside the drift chamber, we have for the drift velocity at a distance z from the orifice

$$u(z)=\frac{u_0R_o^2}{(R_o+z\tan\alpha)^2}, \tag{5}$$

where u_0 is the drift velocity of the flow at the orifice inside the drift chamber. Introducing the parameter

$$\xi=1+\frac{z\tan\alpha}{R_o}, \tag{6}$$

and from the solution of Eq. (5),

$$u(z)=-\frac{dz}{dt}=\frac{u_o}{\xi^2},$$

we obtain the following time dependence for the parameter ξ:

$$\xi^3=\frac{t_o-t}{\tau_o} \quad \text{and} \quad \tau_o=\frac{R_o}{3u_o\tan\alpha}, \tag{7}$$

and for the flow velocity $u(t)$

$$u(t)=u_0\left(\frac{\tau_0}{t_0-t}\right)^{2/3}. \tag{8}$$

Here t varies from zero when $\xi=\xi_o$ up to $t_o-\tau_o$, when $\xi=1$. In particular, for parameters of the argon flow $\alpha=45°$, $R_o=3$ mm, $u_0=2.2\times 10^4$ cm/s we have $\tau_o=4.5\times 10^{-6}$ s. In the case $\alpha=15°$ we get $\tau_0=1.7\times 10^{-5}$ s.

Next we consider the flux of clusters which are located in a gas flow in a cone tube, so that the flow velocity $u(z)$ varies along the tube axis z. For a small cluster concentration when clusters do not act on the flow and do not interact with each other, we will find the equation for drift velocity u of clusters, starting from the Boltzmann kinetic equation for clusters in a buffer gas flow that has the form

$$\frac{\partial f(\mathbf{v})}{\partial t}=\int [f(\mathbf{v}')\varphi(\mathbf{v}_1')-f(\mathbf{v})\varphi(\mathbf{v}_1)]d\sigma d\mathbf{v}_1.$$

Here $f(\mathbf{v})$ is the velocity distribution function for clusters, $\varphi(\mathbf{v}_1)$ is the velocity distribution function for atoms, $\mathbf{v}$ and $\mathbf{v}_1$ are the cluster and atom velocities prior to the collision, while $\mathbf{v}'$ and $\mathbf{v}_1'$ are the cluster and atom velocities after collision, $\mathbf{g}=\mathbf{v}_1-\mathbf{v}$ is the relative velocity during atom-cluster collisions, and $d\sigma$ is the differential cross section of elastic atom-cluster collision that leads to a given variation of velocities.

Multiplying this equation by the cluster momentum $M\mathbf{v}$, where M is the cluster mass, and integrating over the cluster velocities, we obtain the equation for the average cluster momentum $\mathbf{P}=\int M\mathbf{v}f(\mathbf{v})d\mathbf{v}$

$$N_{cl}\frac{d\mathbf{P}}{dt}=\int \mu\mathbf{g}f(\mathbf{v})\varphi(\mathbf{v}_1)\sigma^*(g)d\mathbf{v}d\mathbf{v}_1. \tag{9}$$

Here N_{cl} is the number density of clusters (the distribution functions are normalized by the number densities of corresponding particles), $\mu=Mm/(M+m)$ is the reduced atom-cluster mass (m is the atom mass), and $\sigma^*(g)=\int(1-\cos\vartheta)d\sigma$ is the transport cross section for elastic atom-cluster scattering.

We now see that the cluster mass is relatively large ($M\gg m$), i.e., $\mu=m$, and correspondingly, the cluster distribution function is relatively narrow. This allows us to use the following expression for the cluster velocity distribution function:

$$f(\mathbf{v})=N_{cl}\delta(\mathbf{v}-\mathbf{w}),$$

where $\mathbf{w}$ is the cluster drift velocity, and with Eq. (9) taking the form

$$\frac{d\mathbf{w}}{dt}=\frac{m}{M}N\bar{v}\sigma(\mathbf{u}-\mathbf{w})=\nu(\mathbf{u}-\mathbf{w}) \quad \text{with } \nu=\frac{m}{M}N\bar{v}\sigma. \tag{10}$$

Here N is the number density of atoms, $\bar{v}=\sqrt{8T/(\pi m)}$ is the average atom velocity, $\sigma=\pi r_0^2$ is the cluster cross section, r_0 is the cluster radius, $\mathbf{u}$ is the flow velocity (i.e., the drift velocity of carrier gas atoms) at a given point. In the case $\mathbf{u}=$const the solution of Eq. (10) gives

$$\mathbf{w}=\mathbf{w}_o+(\mathbf{u}-\mathbf{w}_o)\exp\left(-\frac{m}{M}N\bar{v}\sigma t\right),$$

where $\mathbf{w}_o$ is the cluster drift velocity at the beginning. Thus, an equilibrium drift velocity of clusters is established after $\sim M/m$ collisions with buffer gas atoms.

In the case of a carrier gas effusing through a conic tube with azimuthal symmetry, the drift velocity of a buffer gas

varies along the tube such that the rate of atoms passing through each cross section is conserved, and the drift velocity of a buffer gas varies according to formula (5). We use this expression in Eq. (10) that has the form

$$\frac{dw}{dt} + \nu w = \nu u. \tag{11}$$

In particular, for silver clusters of size $n=7000$ that corresponds to experimental conditions (see Fig. 3) and at the pressure of $p=0.12$ mbar and temperature of $T=200$ K ($N=5\times10^{15}$ cm^{-3}) we have $\nu=2.5\times10^3$/s. At the beginning the cluster drift velocity coincides with the atom drift velocity, i.e.,

$$w(0) = u(0) = \frac{u_o \tau_o^{2/3}}{t_o^{2/3}},$$

where τ_o is determined by formula (7) and the drift velocity of buffer gas as function of time given by Eq. (8). Substituting this result into Eq. (11), we obtain

$$\frac{d}{dt}(e^{\nu t} w) = \nu u e^{\nu t} = \frac{\nu u_o \tau_o^{2/3}}{(t_o - t)^{2/3}} e^{\nu t}.$$

Assuming the initial drift velocity of clusters and buffer gas atoms to be zero, the solution of this equation takes the form

$$w(t) = \nu u_o \tau_o^{2/3} e^{-\nu t} \int_0^t \frac{e^{\nu t' dt'}}{(t_o - t')^{2/3}} = \nu u_0 \tau^{2/3} \int_0^t d\tau \frac{\exp(-\nu\tau)}{(\tau + \tau_0)^{2/3}} \tag{12}$$

with the new variable $\tau=t'-t$. The condition of small initial drift velocities of clusters and buffer gas atoms compared to the values near the orifice corresponds to $\nu\tau_0 \ll 1$, that is true in reality. Then we have for the drift velocity of clusters at an orifice

$$w_o = u_o(\nu\tau_o)^{2/3}\Gamma\left(\frac{1}{3}\right) = 2.68 u_o(\nu\tau_o)^{2/3}. \tag{13}$$

Thus, in this limit the equilibrium between the drift velocity of clusters and buffer gas atoms is violated, and the drift velocity of clusters near an orifice is smaller than the flow velocity. Equation (12) allows us to find the cluster drift velocity near the orifice. In particular, under the mentioned experimental parameters and for $\alpha=45°$ Eq. (13) yields $w_o/u_0=0.13$ and $w_o=3\times10^3$ cm/s; for $\alpha=15°$ we obtain $w_o/u_0=0.33$ and $w_o=7.2\times10^3$ cm/s.

One can repeat the deduction for the case of wedge-shaped walls if the buffer gas flows through a rectangular gap instead of a circular orifice. Let us assume that the buffer gas flows between two planar plates which form an angle α with the normal to a gap. Then instead of Eq. (7) we obtain from the solution of Eq. (5),

$$\xi^2 = \frac{t_o - t}{\tau_o}, \quad \tau_o = \frac{l}{4u_o \tan\alpha}, \tag{14}$$

and the flow velocity $u(t)$ becomes equal to

$$u(t) = u_o\left(\frac{\tau_o}{t_o - t}\right)^{1/2}. \tag{15}$$

This gives for the drift velocity of clusters at the gap

$$w_o = u_o(\nu\tau_o)^{2/3}\Gamma\left(\frac{1}{2}\right) = u_o\sqrt{\pi}(\nu\tau_o)^{2/3}. \tag{16}$$

If we take the parameters $\alpha=45°$, $l=3$ mm, $u_o=2.2\times10^4$ cm/s, formula (16) yields $w_o/u_o=0.16$, and $w_o=3.6\times10^3$ cm/s; in the case $\alpha=15°$ we obtain $w_o/u_o=0.32$, and $w_o=7.0\times10^3$ cm/s.

IV. ATTACHMENT OF CHARGED CLUSTERS TO WALLS

We now analyze the attachment of clusters to the walls of the drift chamber. Let us consider a charged cluster being located in a gas near a charged wall that repulses the cluster. The diffusion coefficient of the cluster in a gas is D, and the diffusion of clusters leads to their attachment to walls, if a cluster is located long enough inside the drift chamber. In order to prevent this, an electric field acts on the cluster that repulses a charged cluster from walls to the center. We will characterize this by the cluster drift velocity w to the center, as our task is to find the probability $P(x_o,t)$ for the cluster to attach to walls if at the beginning it is located at a distance x_o from the walls. This distance x_o is small compared to the radius of the wall curvature r that allows us to consider a wall to be plane, reducing it to a one-dimensional problem.

If the probability for a cluster location at time t is at a distance x from the walls, with the boundary condition $P(0,t)=0$, we can express $P(x,t)$ as [22,23]

$$P(x,t) = \frac{1}{4(\pi D t)^{1/2}}\left[\exp\left(-\frac{(x - x_o - wt)^2}{4Dt}\right) - \exp\left(-\frac{(x + x_o + wt)^2}{4Dt}\right)\right]. \tag{17}$$

This gives for the cluster flux to the boundary

$$j = -D\frac{\partial P(x,t)}{\partial x} = \frac{x_o + wt}{4(\pi D)^{1/2} t^{3/2}} \exp\left(-\frac{(x_o + wt)^2}{4Dt}\right), \tag{18}$$

and the probability W of cluster attachment to walls (assuming attachment to take place if the cluster coordinate reaches the value $x=0$),

$$W = \int_0^\infty \frac{x_o + wt}{4(\pi D)^{1/2}} \frac{dt}{t^{3/2}} \exp\left(-\frac{(x_o + wt)^2}{4Dt}\right). \tag{19}$$

Introducing the reduced parameter $\eta=x_o w/(4D)$ and the reduced variable $\tau=wt/x_o$, we may represent this expression in the form

$$W(\eta) = \sqrt{\frac{\eta}{\pi}} \int_0^\infty \frac{(1+\tau)d\tau}{\tau^{3/2}} \exp\left(-\frac{\eta(1+\tau)^2}{\tau}\right). \tag{20}$$

The integral is approximated by

$$W(\eta) = \exp(-4\eta) = \exp\left(-\frac{x_o}{D}\right). \tag{21}$$

It follows that the probability of cluster attachment to walls is unity in the absence of external radial fields if the cluster resides long enough inside the drift tube and moves as a result of diffusion. Next, assuming the electric field strength E to be relatively small, we have for the cluster drift velocity near a charged wall $w=eE|Z|K$, where Z is the cluster charge, and because the cluster mobility K is connected with its diffusion coefficient D by the Einstein relation $K=eD/T$, we get from Eq. (21),

$$W = \exp\left(-\frac{eE|Z|x_o w}{T}\right). \tag{22}$$

Let us make an estimate on the basis of this equation. We assume that the voltage is created by charged rings inside the drift chamber. The voltage of an isolated ring is given by

$$\varphi = \frac{\pi q e R}{\ln \frac{8R}{a}},$$

where R is the ring radius, a is the rod radius, qe is the total charge on the ring, and the electric field strength near the ring on a distance $x \ll R$ is

$$eEx = ex\frac{qe}{2\pi R x} = \frac{\varphi}{4\pi \ln \frac{8R}{a}}.$$

Under experimental conditions ($T=200$ K, $\varphi \sim 100$ V, $R/a \sim 100$, $|Z| \sim 1$) we obtain, with Eq. (22),

$$\frac{eE|Z|x_o w}{T} \sim 50,$$

and attachment of clusters to walls is practically absent under these conditions. Thus, an electrical voltage applied to the walls may prevent the attachment of charged clusters to the walls.

V. PROCESSES INVOLVING CHARGED CLUSTERS IN SECONDARY PLASMA

The above analysis shows that using charged clusters and applying a voltage to the walls, one can prevent clusters from their attachment to the walls. In order to realize this, it is necessary to create a plasma of a low density that can be a secondary plasma of magnetron discharge. This secondary plasma may be a tail of a magnetron plasma, as it was shown in experiment [24]. In this plasma electrons and ions attach to the walls, and the density of charged particles is lower compared to the basic plasma. Because of a higher mobility, electrons attach to walls faster than ions do. As a result, this plasma may be unipolar, with different electron N_e and positive ion N_i number densities ($N_e < N_i$). We consider charging of clusters in such a plasma where the temperatures of charged particles coincide with the gas one T, and this temperature is low (under experimental conditions, $T \approx 200$ K).

Cluster charging results from electron and ion attachment to the cluster surface according to the processes

$$e + M_n \to M_n^-, \quad e + M_n^+ \to M_n, \quad A^+ + M_n \to M_n^+, \quad A^+ + M_n^- \to M_n, \tag{23}$$

where M_n is a cluster consisting of n atoms, e is an electron, A^+ is a positive ion. We neglect the processes

$$e + M_n^- \to M_n^{-2}, \quad A^+ + M_n^+ \to M_n^{+2} \tag{24}$$

because of a strong interaction if an electron or ion are contacted with the cluster surface. In particular, under typical experimental conditions when $T=200$ K, the number of atoms in a silver cluster $n=7\times10^3$ (i.e., a cluster radius is $r_o=3.1$ nm) we have $z_o=e^2/r_oT \approx 27$. Thus, under these conditions clusters may be neutral and singly charged.

In accounting for the processes (23), we have to balance equations for the number densities of neutral N_0, positively N_+ and negatively charged N_- clusters,

$$\frac{dN_0}{dt} = -k_{0,-1}N_eN_0 - k_{0,+1}N_iN_0 + k_{-1,0}N_iN_- + k_{+1,0}N_eN_+, \tag{25}$$

$$\frac{dN_+}{dt} = -k_{+1,0}N_eN_+ + k_{0,+1}N_iN_0,$$

$$\frac{dN_-}{dt} = -k_{-1,0}N_iN_- + k_{0,-1}N_eN_0, \tag{26}$$

where $k_{i,j}$ is the rate constant of change of the cluster charge from i to j. One can express these rate constants through the rate constants of electron k_e and ion k_i collisions with neutral clusters,

$$k_e = \sqrt{\frac{8T}{\pi m_e}}\pi r_o^2 \approx 2.5\times10^{-6}\ \mathrm{cm^3/s}, \quad k_i = \sqrt{\frac{8T}{\pi m_i}}\pi r_o^2 \approx 1.2\times10^{-8}\ \mathrm{cm^3/s}. \tag{27}$$

We take the cross section of attachment to a neutral silver cluster of an average size $r_o=3.1$ nm to be $\pi r_o^2=3\times10^{-13}$ cm^2, m_e, m_i are the electron and argon ion masses, and the temperature is taken to be $T=200$ K. The rate constants of the balance equations (25) and (26) are expressed through these rates on the basis of the relations [25]

$$k_{0,-1}=k_e, \quad k_{0,+1}=k_i, \quad k_{+1,0}=k_e(1+z_o), \quad k_{-1,0}=k_i(1+z_o). \tag{28}$$

Solving stationary balance equations (25) and (26) with taking into account these rate constants, we obtain $N_e/N_i=4\times10^{-3}$ for this experiment,

$$\frac{N_-}{N_0} = \frac{k_e}{k_i(1+z_o)}\frac{N_e}{N_i}, \quad \frac{N_+}{N_0} = \frac{k_i}{k_e(1+z_o)}\frac{N_i}{N_e}. \tag{29}$$

We use these relations for treatment of this experiment according to which the ratio of currents of positively and negatively charged clusters is approximately 1.5. Taking $N_+/N_-=1.5$, we obtain from Eqs. (29),

$$\frac{N_+}{N_-} = \left(\frac{k_i N_i}{k_e N_e}\right)^2 = 1.5. \tag{30}$$

Using the rate constants (27) under experimental conditions, we obtain for a unipolar secondary plasma near the orifice

$$\frac{N_e}{N_i} = 4 \times 10^{-3}.$$

Thus, the secondary plasma with clusters is a unipolar plasma near the orifice of the magnetron chamber, so that most of the electrons are attached to walls. A typical time for establishment of this equilibrium is $\tau \sim 10^{-2}$ s for $N_i \sim 10^{10}$ cm^{-3}. Let us compare this time with a typical drift time. Considering a flow of a buffer gas with clusters in a cone tube, we have for the drift time

$$\tau_{dr} = \int_R^{r_o} \frac{dzR^2}{u_0 r_o^2} = \frac{R^3}{3 \tan \alpha u_0 r_o^2}.$$

Taking under experimental conditions $R=5$ cm, $\alpha=45°$, $r_o=3$ mm, $u_0=2.2\times10^4$ cm/s, we obtain $\tau_{dr}=0.02$ s, i.e., it is comparable with a time of establishment for charge equilibrium of clusters.

These estimations show a nonequilibrium character of electric processes in the secondary plasma with clusters. As electrons go and attach to the walls, the secondary plasma becomes unipolar and contains mostly positive ions. Correspondingly, a typical time of establishment of the charge equilibrium for clusters increases. If the number density of positive ions is less significant than $N_i \sim 10^{10}$ cm^{-3}, the cluster charge is frozen at values when the ion number density is of the order of this magnitude. Thus, the processes of cluster charging may be nonequilibrium in the secondary magnetron plasma.

Coagulation of clusters in secondary plasma. We convince in a nonequilibrium character of various equilibria in a flow magnetron cluster plasma. First, near the orifice the drift velocity of a buffer gas differs from that of clusters by an order of magnitude for our experimental conditions. Second, this plasma becomes unipolar because of an electron departure from the secondary plasma. As a result, clusters may be positive and negative, and in this experiment numbers of neutral, positive, and negative clusters are comparable. Thus near the orifice the number density of clusters increases because of different drift velocity compared with that of a buffer gas and also these clusters can have different charge sign. This accelerates the coagulation process near the orifice, and we estimate below a cluster size increase due to the coagulation process.

These estimations will be based on general methods of the coagulation analysis for aerosols and clusters [25–27]. But the dependence of the rate constant of cluster joining $k_n \sim n^{-1/6}$ on the number n of cluster atoms differs from the considered case. This dependence leads to the loss of small clusters, and a typical rate constant of joining of two clusters is $k_n \sim 1\times10^{-7}$ cm^3/s for silver clusters under typical experimental conditions ($T=200$ K, $n=7\times10^3$, $r_o=3.1$ nm). Taking the number density of clusters in the orifice region $N_{cl} \sim 10^8$ cm^{-3} that corresponds to the cluster current $J \simeq 10^{-8}$ g/s for this experiment, we obtain for a typical time $\tau_{\text{coag}} \sim 0.1$ s for cluster growth by coagulation. Though this value is smaller than the drifting time, the coagulation process may influence the cluster distribution function. Moreover, this process can change the size distribution function of clusters by a decrease of small clusters.

VI. OUTLET OF FLOW WITH CLUSTERS FROM MAGNETRON CHAMBER

We conclude that averting of cluster attachment to walls requires charging of clusters and voltage of walls with respect to a flow with clusters. Let us assume it is fulfilled and then charged clusters inside a flow of buffer gas leave the magnetron chamber through an orifice or a gap. Evidently, optimal conditions allowed to escape cluster attachment to an orifice or walls near the orifice require to give an electric voltage to an orifice. But if the number density of charged clusters is not small and the orifice voltage is restricted, an electric field of an orifice is not able to keep charged clusters in a flow and an excess of clusters will attach to walls near the orifice. Hence, an orifice is able to pass a certain flux of charged clusters, and we below estimate this value.

We assume for simplicity that electrons and ions of a plasma attach to walls, and a buffer gas flow contains only singly charged clusters. The behavior of this system near a round orifice is governed by the Poisson equation. From the solution of the Poisson equation it follows that a voltage of a unipolar plasma is

$$\varphi_o = \pi e N_i r_o^2, \tag{31}$$

if we assume the cluster plasma to be uniform. Evidently, this plasma is steady in the field of the orifice, i.e., charged particles do not move to walls, if

$$\varphi_o \leqslant V_o,$$

where V_o is the orifice voltage with respect to a plasma flow. From this it follows the condition of plasma stability,

$$eN_i \pi r_o^2 \leqslant V_o,$$

and this is fulfilled not only near the orifice, but in each cross section, so that an excess of charges attaches to the walls. This gives the following restriction for the total rate of clusters which leave the magnetron chamber

$$J = m_{cl} w_{cl} N_i \pi r_o^2 \leqslant m_{cl} w_{cl} V_o / e, \tag{32}$$

where m_{cl} is the mean mass of individual cluster, w_{cl} is the cluster drift velocity near the orifice, and the rate J is the metal mass per unit time that leaves the magnetron chamber per unit time. As is seen, the latter is independent of the orifice radius.

Let us make some estimate for the following experimental conditions: an electric potential of $V_o=200$ eV at the orifice, singly-charged clusters with size $n=7000$ in accordance with Fig. 3 ($m_{cl}=1.2\times10^{-18}$ g). The drift velocity of clusters is taken to be $w_{cl}=3\times10^3$ cm/s that corresponds to the conic shape of the magnetron chamber near the orifice with an angle $\alpha=45°$. This gives for the total rate of silver clusters

5×10^{-6} g/s that provides the growth rate of a silver film of ~1 μm/min deposited on a target of an area of several cm^2.

Let us compare this rate of the silver flow with the possibility of the above magnetron discharge whose mean power is 120 W (see Fig. 3). Taking the formation efficiency (sputtering yield) of a silver atom to be 0.37 [28,29] at an ion energy of 250 eV, we find the energy cost of one silver atom to be about 700 eV. Then this discharge can provide the rate of silver atoms to be of 2×10^{-4} g/s. As it is seen, only 2% of evaporated atoms are able to pass through the orifice in the form of clusters under the above conditions. Of course, the most part of initially released metal atoms returns back to the cathode. But evidently a remarkable part of metallic atoms formed clusters attached to the walls of the magnetron chamber.

In order to prevent attachment of clusters to walls, it is convenient to use a gap for outlet of a flow instead of the orifice and a wedge shape of the magnetron chamber near the gap. Denote the gap depth by d and the gap length by l, and $l \gg d$. We then obtain for the potential difference between the gap center and its edge due to charged clusters in the following formula:

$$\varphi_o = \frac{\pi}{2} e N_t d^2$$

instead of (31). Correspondingly, we have for the rate of the metal flow,

$$J = m_{cl} w_{cl} d l N_{cl} \leqslant \frac{2l}{\pi d e} m_{cl} w_{cl} V_o \tag{33}$$

instead of (32). As follows from this formula, the flow rate for charged clusters can be increased by an increase of the gap length.

From this analysis we obtain the following conclusion. Optimizing the regime of the buffer gas flow with clusters far from the cathode, it is necessary to prevent clusters from attachment by cluster charging and applying an electric voltage to walls near the orifice. For a round orifice this voltage for a given cluster rate is independent of the orifice and increases with an increase of the cluster flow rate. But in practice the wall voltage is restricted, say, by several hundred volts, and this voltage is not enough to provide metal fluxes in clusters under optimal conditions. This trouble can be overcome by using an oblong orifice.

VII. CONCLUSION

Metal clusters are generated effectively under the action of a magnetron discharge with a large efficiency for sputtering of metal atoms. Due to the low gas density, metal atoms and clusters can attach to wall of the drift chamber. In order to prevent this, one can use charging of clusters in the secondary plasma of magnetron discharge that exists far from the cathode. Then if these clusters obtain an identical charge, a voltage of walls near the orifice does not allow cluster attachment to the walls. An experimental analysis of this paper confirms charging of clusters in the secondary plasma.

Another force acting on clusters from a buffer gas flow delays clusters in a flow and increases their number density in the drift chamber near an orifice through which a buffer gas with clusters leaves the magnetron chamber. This leads to an increase of the number density of clusters and intensifies the coagulation process involving neutral clusters.

Considering this problem as a whole, we note that magnetron discharge provides a high efficiency of generation of metal atoms as a result of bombardment of the cathode by discharge ions. These metal atoms return mostly to the cathode or attach to walls. Using a buffer gas flow, one can convert metal atoms partially into metal clusters that leads to a decrease of metal losses as a result of its attachment to walls. Nevertheless, if metal clusters are removed from the magnetron chamber through an orifice, one can decrease the rate of metal attachment to walls by applying a voltage to the walls and by simultaneous charging of clusters. Then clusters are repulsed from the walls, that increases the metal yield in clusters located in a carrier gas flow.

On this way from this experimental study and theoretical analysis of the magnetron cluster plasma under these experimental conditions we convince a nonequilibrium character of evolution of the magnetron cluster plasma far from the cathode. This results both in an increase of the cluster number density in the orifice region and in formation of unipolar plasma in this region with a small electron concentration. One can use these processes in order to increase the cluster yield from the magnetron plasma. Then it is necessary to satisfy the following requirements. First, a soft transition is required from the magnetron chamber to the orifice, for example, the cone shape of the magnetron chamber near the orifice in contrast to standard chamber construction with an orifice in a cylinder tube. This will provide a laminar flow near walls while turbulent flows lead to additional cluster attachment to walls. Second, the walls consist of sections with certain voltages. This allows one to operate both the secondary plasma with cluster charging processes and the character of a flow of charged clusters through the orifice. Third, under optimal conditions of cluster yield with high cluster fluxes the orifice must have an oblong shape or a gap shape that decreases the orifice voltage. Note that though we keep in the above analysis experimental conditions, these conclusions have a general character.

Thus, this experimental and theoretical analysis shows a complex character of processes in a magnetron cluster plasma which determine the cluster yield. Understanding and operating by these processes allows one to improve the yield parameters of this cluster source.

ACKNOWLEDGMENTS

Part of this work was supported by the Deutsche Forschungsgemeinschaft (DFG) through Sonderforschungsbereich SFB/TR 24 *Fundamentals of Complex Plasmas*. One of the authors (B.M.S.) thanks RFBR (Grant No. 06-02-16146) for partial support.

[1] B. M. Smirnov, Phys. Usp. **43**, 453 (2000).
[2] B. M. Smirnov, Phys. Usp. **46**, 589 (2003).
[3] B. M. Smirnov, Contrib. Plasma Phys. **44**, 558 (2004).
[4] R. E. Smalley, Laser Chem. **2**, 167 (1983).
[5] J. B. Hopkins, P. R. R. Langridge-Smith, M. D. Morse, and R. E. Smalley, J. Chem. Phys. **78**, 1627 (1983).
[6] S. H. Yang, C. L. Pettiette, J. Conceicao, O. Cheshnovsky, and R. E. Smalley, Chem. Phys. Lett. **139**, 233 (1987); O. Cheshnovsky, S. H. Yang, C. L. Pettiette, M. J. Craycraft, and R. E. Smalley, Rev. Sci. Instrum. **58**, 2131 (1987).
[7] P. Milany and W. A. de Heer, Rev. Sci. Instrum. **61**, 1835 (1990).
[8] H. Haberland, M. Karrais, M. Mall, and Y. Thurner, J. Vac. Sci. Technol. A **10**, 3266 (1992).
[9] H. Haberland, Z. Insepov, M. Karrais, M. Mall, M. Moseler, and Y. Thurner, Mater. Sci. Eng., B **19**, 31 (1993).
[10] H. Haberland, M. Moseler, Y. Qiang, O. Rattunde, T. Reiners, and Y. Thurner, Surf. Rev. Lett. **3**, 887 (1996).
[11] I. Shyjumon, M. Gopinadhan, C. A. Helm, B. M. Smirnov, and R. Hippler, Thin Solid Films **500**, 41 (2006).
[12] S. Pratontep, S. J. Carroll, C. Xirouchaki, M. Streun, and R. E. Palmer, Rev. Sci. Instrum. **76**, 045103 (2005).
[13] H. Haberland, *Clusters of Atoms and Molecules* (Springer-Verlag, New York, 1994).
[14] H. Haberland, B. von Issendorff, J. Yufeng, and T. Kolar, Phys. Rev. Lett. **69**, 3212 (1992).
[15] H. Haberland, M. Mall, M. Moseler, Y. Qiang, T. Reiners, and Y. Thurner, J. Vac. Sci. Technol. A **12**, 2925 (1994).
[16] J. R. Roth, *Industrial Plasma Engineering, Vol.2, Applications to Nonthermal Plasma Processing* (IOP, Bristol, 2001).
[17] P. Baroch, J. Musil, J. Vlcek, K. H. Nam, and J. G. Han, Surf. Coat. Technol. **193**, 107 (2005).
[18] Quadrupole mass filter—QMF 200, Oxford applied research, version 1.1.
[19] *Atomic and Molecular Beam Methods*, edited by G. Scoles (Oxford University Press, Oxford, 1988), Vol. 1, Chap. 8.
[20] I. Shyjumon, M. Gopinadhan, O. Ivanova, M. Quaas, H. Wulff, C. A. Helm, and R. Hippler, Eur. Phys. J. D **37**, 409 (2006).
[21] C. Cui and J. Goree, IEEE Trans. Plasma Sci. **22**, 151 (1994).
[22] L. D. Landau and E. M. Lifshitz, *Fluid Dynamics* (Pergamon, Oxford, 1986).
[23] B. M. Smirnov, *Physics of Ionized Gases* (Wiley, New York, 2001).
[24] R. Hippler, S. Wrehde, V. Stranak, O. Zhigalov, H. Steffen, M. Tichy, M. Quaas, and H. Wulff, Contrib. Plasma Phys. **45**, 348 (2005).
[25] B. M. Smirnov, *Clusters and Small Particles in Gases and Plasmas* (Springer, New York, 2000).
[26] V. M. Voloshchuk, *Kinetic Theory of Coagulation* (Hidrometeoizdat, Leningrad, 1984).
[27] I. Gutzov and J. Schmelzer, *The Vitreous State* (Springer, Berlin, 1995).
[28] D. Samsonov and J. Goree, J. Vac. Sci. Technol. A **17**, 2835 (1999).
[29] D. Samsonov and J. Goree, Phys. Rev. E **59**, 1047 (1999).